International Journal of Nanoelectronics and Materials
IJNeaM
ISSN 1985-5761 | E-ISSN 2232-1535

A Synthesis and Comparative Study of the Performance of Polyacrylonitrile-Fe_2O_3 and TiO_2 Nanocomposite Membranes for Crude Oil/Water Separation

Hassan Yassin Taha, Omar S. Dahham*

Department of Chemical Engineering, College of Engineering, University of Baghdad, Baghdad, Iraq.
**Corresponding author. E-mail: omar.s@coeng.uobaghdad.edu.iq*

ABSTRACT

Due to the strong absorption and three-dimensional structure of the 8 wt% PAN-Fe_2O_3 and PAN-TiO_2 nanocomposite films, an aqueous solution polymerization was used to create a photodegradable composite with N-methyl-2-pyrrolidone (NMP) as a crosslinking agent. Fourier transform infrared spectroscopy (FTIR) was used to determine which groups in the composite are active. The contact angles were measured for different concentrations of the 8 wt% PAN-Fe_2O_3 and PAN-TiO_2 nanocomposite films. In addition, a scanning electron microscope (SEM) was used to understand the morphological characteristics of the composites. Gas chromatography (GC) was used to evaluate the efficiency of oil/water separation. The optimal separation time was at 5 min, after which the removal efficiency decreased with the 8 wt% PAN-Fe_2O_3 concentration. The optimum efficiency of removal was achieved on the PAN-TiO_2 surface at 8 wt% concentration and reached to 98% at 10 g/90 ml (10%) crude oil/water concentration, this is due to the high hydrophilic tendency 8 wt% PAN-TiO_2 . The nanocomposite membranes with 8 wt% PAN-Fe_2O_3 and PAN-TiO_2, are easy to fabricate, have low component costs, are robust, and offer high performance, which have great potential for industrial-scale applications in the treatment of oily industrial wastewater in harsh environments.

Keywords: *Nanocomposite Membranes, Crude Oil /Water Separation, Contact Angle Measurements, Polyacrylonitrile Films*

1. INTRODUCTION

We There are both liquid and solid parts to oil refinery waste. Many industries are required to separate oil and water to avoid waste and obey environmental guidelines. As well as the usual approaches now being used, we should develop new and more modern technologies to address this issue. Due to frequent oil spills and oily wastewater from industry, it has become difficult to effectively separate oil from water on a global scale [1]. Currently, Crude Oil /water mixtures can be treated with membrane-based technologies, though they usually have several disadvantages, like requiring costly equipment or a lot of energy [2, 3]. One particularly advantageous feature of using a PAN-based enhancement to a membrane is that the hydrogel so formed has a lower degree of contamination from oil. Other benefits are that residual oil in the separated water has a low concentration and that manufacturing these reinforced hydrogels is very economical.

Branching in a polymer leads to a high degree of cross-linking, and the degree of cross-linking is important to mechanical and thermal properties. Industrial applications of water-soluble hydrophobic polymers include, for example, cosmetics and paints, oil extraction, and drilling fluids are made with hydrophobic alkyl groups on the polymer chain, which help with condensation and air–liquid surface activity. A superabsorbent polymer (SAP) [4] was investigated that is synthesized by suspension reverse polymerization and dilute solution polymerization using acrylamide, acrylic acid, and their salts. [5, 6] These are superabsorbent polymers that can absorb aqueous or water solutions and are used in personal hygiene products. Cross-link density of SAPs rises with increasing cross-link density until an optimum cross-link density is attained, attains a maximum swelling capacity, and then falls off with increasing stainless steel mesh density [7, 8, 9].

The effect of polyacrylonitrile-Fe_2O_3 (PAN-Fe_2O_3) or PAN-TiO_2 nanocomposite membrane concentration on membrane performance was investigated using phase inversion technology with a polyacrylonitrile-Fe_2O_3 or TiO_2 polymer membrane for petroleum refining water separation, achieved by coating with crosslinked Poly (vinyl alcohol) PVA. The concentration of polyacrylonitrile-Fe_2O_3 or TiO_2 nanocomposite membrane can enhance membrane performance by increasing flux and removal rates, as Fe_2O_3 or TiO_2 possess properties that improve hydrophilic characteristics [10].

Isadora et al. (2024) [11] found that the hydrogel-coated structural pad could remove more than 90 percent of the water from the oils and make the oil clearer, brighter, and more transparent. In places where water is polluted, the hydrogel-coated pad helps quickly separate water, which is important for industrial settings. Oils always contain water, and this water is not wanted. Water may get into the product during the production, transportation, or storage stages in the form of dissolved, emulsified, or free water (Teng et al., 2022; Estevam et al., 2023) [12, 13]. In addition, the way liquid films are created and stabilized is influenced by the exact composition of the filler and its order in the cement mix (Blauth et al. 2025) [14].

(Hidayah et al. 2021) [15], reported that the effect of UV exposure duration on the performance of a polyacrylonitrile-Fe_2O_3 nanocomposite membrane for oil refinery wastewater separation resulted in increased membrane flux and decreased rejection value. The addition of PEG to enhance the efficiency and characterization of nanocomposite membranes for oil refinery wastewater separation was further enhanced.

Surkatti et al. (2024) [16] mention that many biomedical fields use Poly (vinyl alcohol) PVA/nanoparticles like Fe_2O_3 and TiO_2, but there are constraints for using them in biomass stabilization. In addition, there are no studies that have looked at different nanoparticles to see how they can improve the properties of hydrogels. Hence, this work looks at using Fe_2O_3 and TiO_2 metal oxide nanoparticles to strengthen PVA gel for biomass stabilization. PVA/metal oxide nanoparticle composites were made by adding a small amount of nanoparticles to a 10 wt% PVA solution. In addition, the impact of nanoparticle type and amount on the appearance and functions of PVA/hydrogel nanoparticle composites was studied. The PVA gel composites were put through a bioreactor and studied against pure PVA gel to see how the matrix held up.

Using nanoparticles (NPs) in polymeric membranes is becoming more common because of their specific features and their involvement in oily wastewater treatment [Salim et al., 2022] [17], as well as their small size and large surface [Lu et al., 2016] [18]. Some of the common inorganic nanoparticles include titanium dioxide (TiO2), ferrous oxide (Fe_3O_4), silicon dioxide (SiO_2), graphene oxide (GO), aluminum oxide (Al_2O_3), carbon nanotubes (CNTs), zirconium dioxide (ZrO_2), silver (Ag), zinc oxide (ZnO), mobile composite material 41 (MCM-41) and oxygen-deficient tungsten oxide (WO2.89) The studies by Al-Jumaili et al. in 2018 [23], 2019 [24] and Amna et al. in 2020 [25], along with Rana et al. in 2021 [26] and Reham et al. in 2022 [27], provide useful information.

In the research, nanoparticles of iron oxide (Fe_3O_4) and titanium dioxide (TiO_2) were manufactured to be used for the creation of nanocomposites. As there is not much research on polyacrylonitrile (PAN): PAN-Fe_2O_3 and PAN-TiO_2 nanocomposite films, this study sought to produce hydrophobic nanocomposites using synthesized titanium dioxide (TiO_2) and iron oxide (Fe_3O_4) nanoparticles, polyurethane beads, and iron dioxide (Fe_2O_3) nanoparticles. Fe_3O_4 and Fe_2O_3 nanoparticles were chosen because they have good magnetic properties that help with hydrophobicity, and titanium dioxide nanoparticles were chosen for their hydrophobicity. The structure, surface look, and thermal stability of the new nanocomposites were studied. The ability of the membrane to repel water, separate oil from water, how effective it is at separating, and if it can be used more than once were also checked.

2. EXPERIMENTAL WORK

2.1. Chemicals and Raw Materials

Polyacrylonitrile (PAN), Nano Fe_2O_3, and TiO_2, N-methyl-pyrrolidone (NMP), Polyethylene glycol 6000 (PEG 6000), and Polyvinyl alcohol (PVA) were purchased from Shanghai Macklin Biochemical Co., Ltd., and UV-Irradiation, Glass plate using a casting knife. Crude oil from the Durra refinery was used; every experiment used deionized water DI. Glass tubes with compression clamps. All materials were used without any preliminary treatment.

2.2. Formulation of 8wt% of Polyacrylonitrile-Fe_2O_3 (PAN-Fe_2O_3) and (PAN-TiO_2) Membrane Nano Composite

The 8wt% (PAN-Fe_2O_3) and (PAN-TiO_2) Membrane Nano Composite. 25 g: At the stage of making polyacrylonitrile films, starting from making a solution and according to Table 1, printing consisting of 5g of polyacrylonitrile as a polymer with a composition of 18% by weight. 2g (8wt%) of nano-Fe_2O_3 or TiO_2 are added. 2g of Polyethylene glycol (PEG) 6000 is used as an additive with compositions for polyacrylonitrile films, and the remainder is used as a solvent, 16g of n-methyl-2-pyrrolidone (NMP). The film printing uses the reversed-phase method. This method involves printing the film onto a glass plate using a casting knife and then immersing the glass plate in a coagulation bath. This research investigates the effect of post-treatment, i.e., temperature. The film with the best performance is then heated to (70-80) ±2°C, its optimum temperature, with heating times of 2 min for polyacrylonitrile. UV light is added for five minutes, as shown in Figure 1. Finally, 3g of polyvinyl alcohol should be added with mixing for 5 min. Put this membrane in the separation system.

Table 1 Formulation of 8wt% of (PAN-Fe_2O_3), and (PAN-TiO_2) Membrane Nano Composite (25g)

Materials	State	Wt. g	Time	Heating
PAN	S	5		
Nano Fe2O3 and TiO2	S	2		
PEG	S	2		
NMP		16 (the rest)		
Polyvinyl alcohol 3%	S	3 g	5 min	80 °c
UV			5 min	
Heating			2 min	70 °c

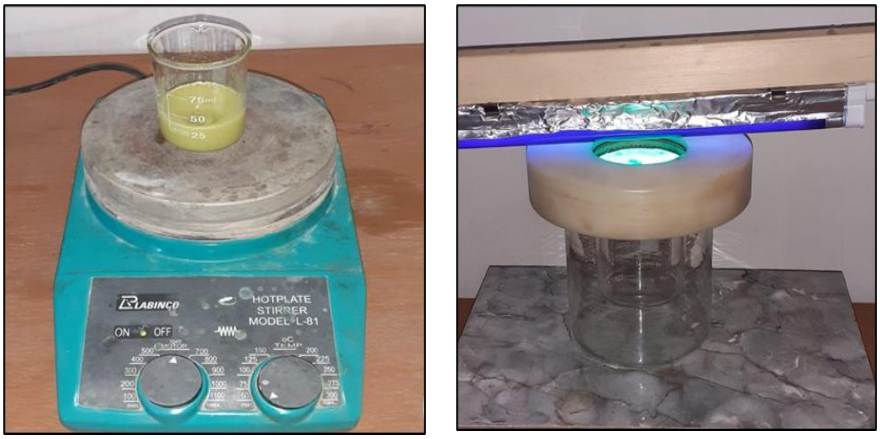

Figure 1. The membrane under UV rays for (PAN-Fe_2O_3) and (PAN-TiO_2) Membrane Nano Composite polyacrylonitrile films.

2.3. Oil / Water Separation Procedure

For the homogeneous mixture, the two components were put into a beaker and stirred at 600 rpm for 15 min to achieve mixtures of oil with different percentages of water (10/90, 25/75, 50/50, 75/25 and 90/10) (Figure. 2a). To set up the filter, we used two graduated glass cylinders with grooves to hold an O-ring that forms an airtight seal with the reinforced membrane (Figure 2b). The upper cylinder has an internal diameter (ID=2.5 cm) into which are poured crude oil/water mixtures, from where, at the bottom of the cylinder, water is collected. Each trial was recorded for a separation time. The crude oil/water mixture drained into the upper cylinder of glass, and oil remained in the glass cylinder.

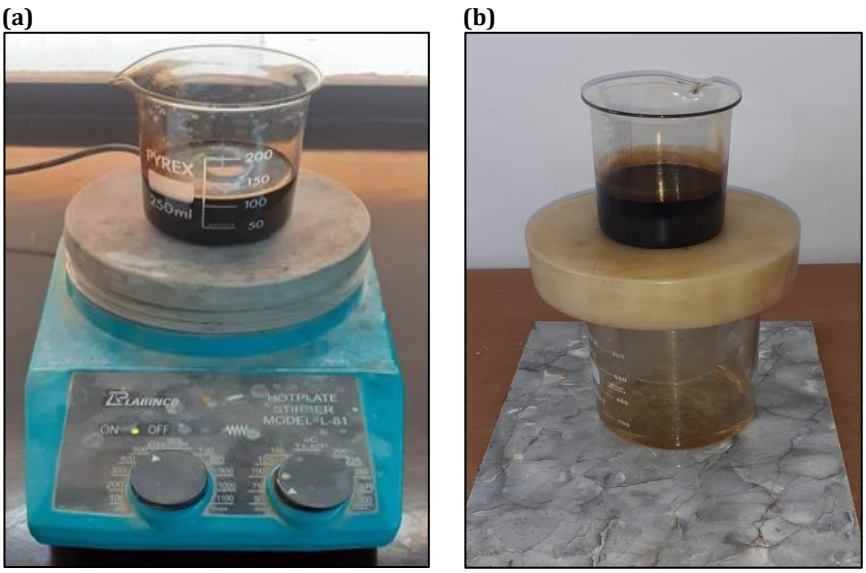

Figure 2. The mixtures of oil/water, (b) Crude oil/ water separation system.

The permeate water has a high separation efficiency (S Eff.) and practically no visible oil in it. Oil content was determined before and after the separation using an infrared spectrometer oil content analyzer. Therefore, the separation efficiency is determined by the oil removal coefficient (R%):

$$\% R = \left(1 - \frac{C_P}{C_O}\right) \times 100 \quad (1)$$

Gas chromatography (GC) is used using C_o and C_p. the oil concentrations of the water are then assessed in the collected water after a one-time separation and in the original oil/water mixture, respectively, where C_o is higher than C_p.

2.4. Characterization

Sample characterization: 8wt% of (PAN-Fe_2O_3) and (PAN-TiO_2) Membrane Nano Composite polyacrylonitrile films were characterized by Fourier Transform Infrared Spectroscopy (FTIR) to determine the effective functional group for the manufacturer material, the calculation of the contact angles of two (PAN-Fe_2O_3) and (PAN-TiO_2) Membrane Nano Composite polyacrylonitrile films concentrations (CA), and Scanning Electron Microscopy (SEM) to give an enlarged and detailed image for the sample. At the same time, Gas chromatography (GC) was used to evaluate the oil/water separation.

3. RESULTS AND DISCUSSIONS

3.1. Characterization

FTIR: Slices measuring 1 cm in diameter and 20 μm thick were made and mixed with potassium bromide. The sample was applied to the slices, which were loaded into the apparatus, and the infrared spectrum was recorded between 400 and 4000 cm-1 at a resolution of 4 cm-1. In both (PAN-Fe_2O_3) and (PAN-TiO_2) Membrane Nano Composite polyacrylonitrile films, the absorption peaks at 3450.7 cm−1 in the PAM spectrum (Figures 3 a and b) suggest O–H stretching, at 3200 cm−1 show N–H bending, at 1474 cm−1 are C=O stretching, at 2800 cm−1 are -CH_2 stretching, at 1312 cm−1 are C–H bending and at In the composite spectrum of (PAN-Fe_2O_3) and (PAN-TiO_2), the peaks at 1384 cm−1 and 1064.1 cm−1 are due to C–O–H deformation vibration and Ti–O–C vibration which indicate that both composites interact with PAN through -OH, as can be seen in Figure 3 [28], [29].

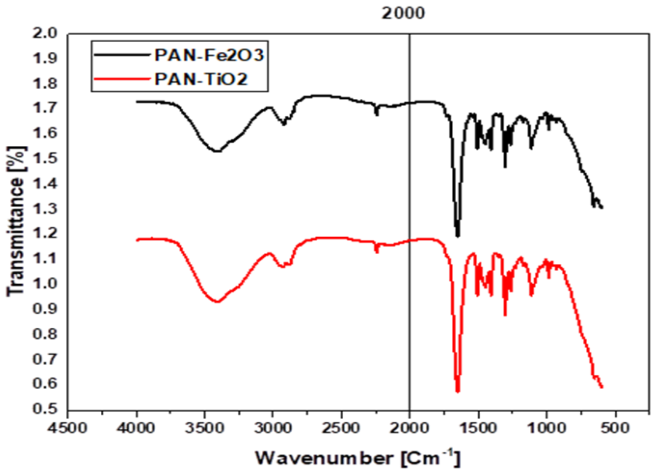

Figure 3. FTIR spectrums for (a) PAN-Fe_2O_3, (b) PAN-TiO_2.

XRD: Figure 4a, b shows the X-ray diffraction patterns of both (PAN-Fe_2O_3) and (PAN-TiO_2). The intensity of the characteristic Fe_2O_3 and TiO_2 peaks increases with increasing TiO_2 loading on the PAN, indicating the incorporation of TiO_2 into the PAN. Detailed results match Figure 2, with 2θ values of 14.05, 19.2, 25.55, 32.6, 37.05, 41.6, 48.9, 54.95, 64.75, and 64.8 for PAN-TiO2. A higher intensity at 2h = 25.4 for TiO2/PAN also means that the PAN has more anatase phase present. The presence of TiO2 in the films brought about a new diffraction peak at 2θ = 26.5 ◦, which was assigned to the (101) crystal planes of TiO2 and supported the incorporation of TiO2 in the PAN films [30]. Also, the Fe_2O_3 XRD spectrum exhibited peak average crystallite sizes of the α-Fe_2O_3 nanocomposites, which were 47.09 nm, respectively. The crystal size calculation results showed that all the materials produced in this study were on the nanoscale [30].

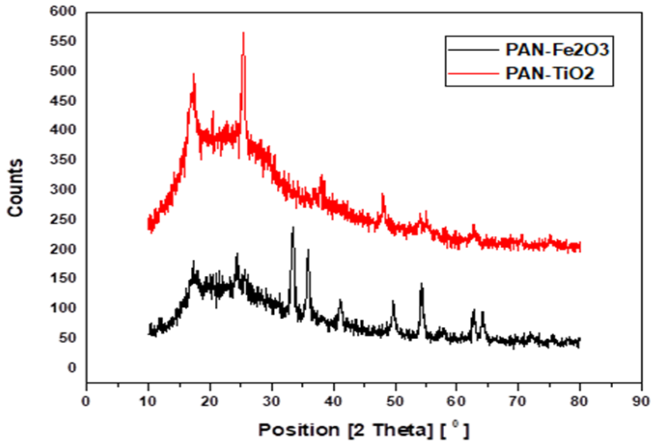

Figure 4. X-ray diffraction patterns for (a) PAN-Fe_2O_3, (b) PAN-TiO_2.

SEM: The membrane surface and cross-sectional structure were analyzed using a scanning electron microscope (SEM). This analysis provides qualitative information about the membrane's pore size, distribution, and overall geometry [16]. The membrane surface can be observed through a scanning electron microscope (SEM), and an image can be captured. Figures 5a and b present the results of SEM image analysis to determine the membrane morphology based on the membrane surface (outer surface) and its cross-sectional structure. Figure 5b indicates that the membrane pores are slightly larger and more uniform. The cross-sectional analysis of the nanocomposite membranes demonstrates that fouling is caused by the presence of inorganic (organic) chemicals and microorganisms. As the fouling flux decreases, the membrane replacement/washing is performed [17].

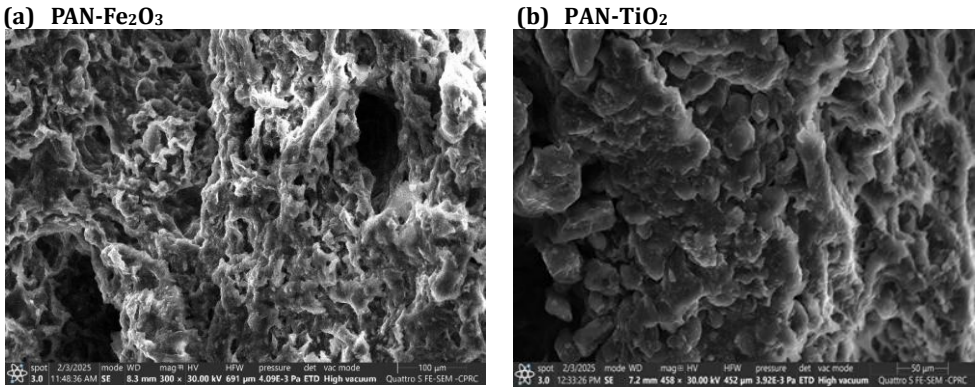

Figure 5. SEM micrographs of (a) PAN-Fe_2O_3, (b) PAN-TiO_2.

Contact Angle: As shown in Figure 6, the difference in the shape of water droplets in air on PAN-Fe_2O_3 and PAN-TiO_2 is evident. The water droplet spread over the nanocomposite polyacrylonitrile membranes and quickly entered the surface of the PAN-TiO_2 membrane, where it was rapidly adsorbed within a few seconds, as illustrated in Figure 6(b). The contact angle was θ=9.6°, whereas in Figure 6(a), the water droplet spread slowly on the membrane surface with a contact angle of approximately θ=26.7°. This indicates that PAN-TiO_2 is highly hydrophilic. All the contact angles of the membrane surface were less than 20. The smaller pores and greater surface roughness, combined with the larger current densities, change the hydrophobicity of the membrane surface, depending on pore size. The area covered by the oil film on the membrane will shrink in cases where the oil film is rougher [31].

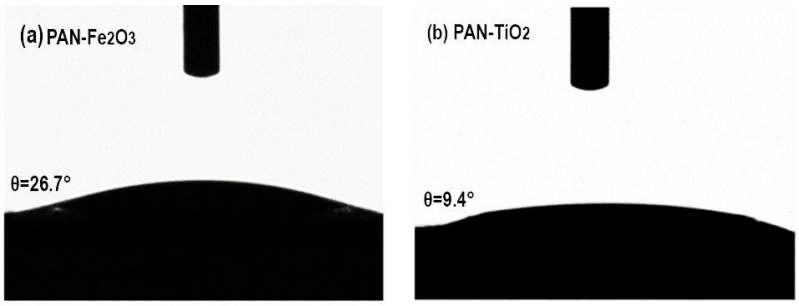

Figure 6. Contact Angles CA analysis of (a) PAN-Fe_2O_3, (b) PAN-TiO_2.

3.2. Study of the Separation Efficiency of (Crude oil/ Water)

Change of Concentration: The crude oil/water concentration (10 wt%, 25 wt%, 50 wt%, 75 wt%, and 90 wt%) varied with PAN-Fe_2O_3 and PAN-TiO_2. The best R was 96.7% at PAN-TiO_2 and 10 wt% crude oil/water. As shown in Figure 7.

Change of Contact Time: The removal of water from an aqueous solution (crude oil/water) depends on the initial crude oil concentration and the contact time. The amount of water removed decreases proportionally as the initial crude oil/water concentration increases. Water removal improves with time, with the optimal duration being 5 minutes. Water removal from aqueous solution (crude oil/water) depends on the initial crude oil concentration and contact time. The amount of water removed decreases proportionally with the initial crude oil/water concentration increase. Water removal improves with time, with the optimum time being 5 min. The crude oil/water concentration (10 wt%, 25 wt%, 50 wt%, 75 wt%, and 90 wt%) was varied with PAN-Fe_2O_3 and PAN-TiO_2. The best R was 98% for PAN-TiO_2 and 10 wt% crude oil/water, as shown in Figure 8, [32, 33].

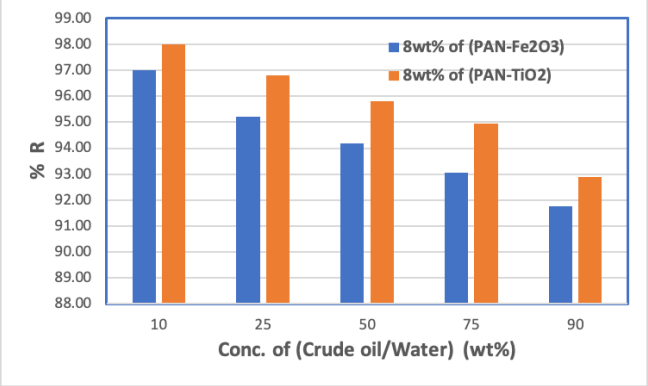

Figure 7. Change of (crude oil/water) concentration with PAN-Fe_2O_3 and PAN-TiO_2.

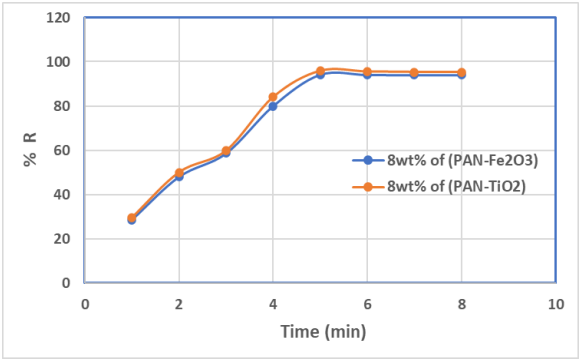

(a)

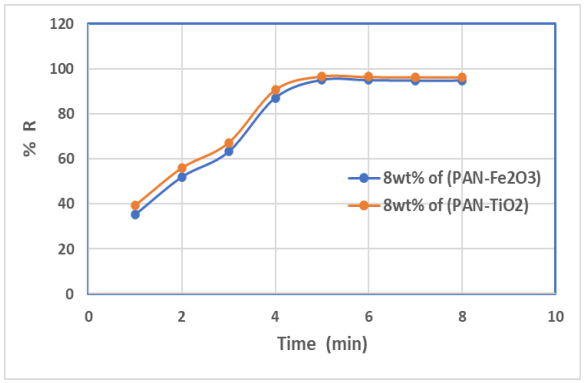

(b)

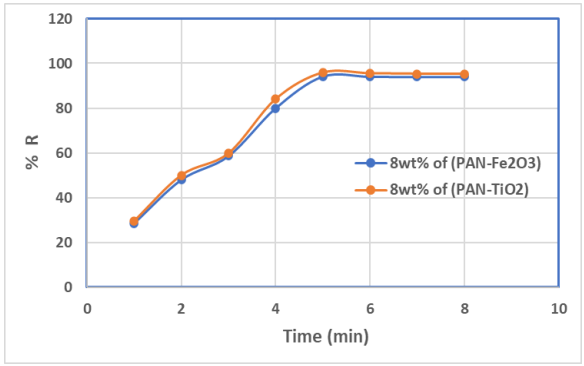

(c)

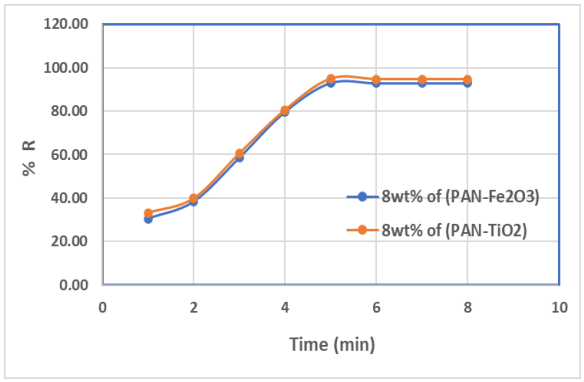

(d)

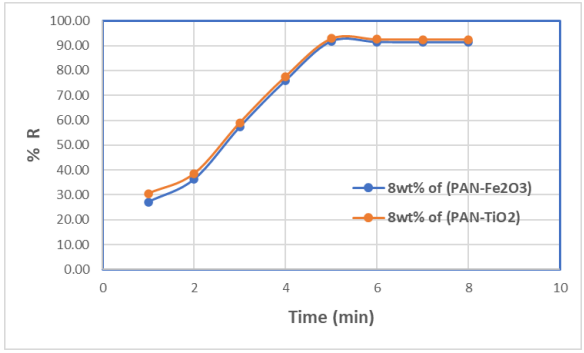

(e)

Figure 8. Change of contact time with changing concentration of (crude oil/water), (a) 10 wt% crude oil/water, (b) 25 wt% crude oil/water, (c) 50 wt% crude oil/water, (d) 75 wt% crude oil/water, and 90 wt% crude oil/water on the surface of PAN-Fe_2O_3 and PAN-TiO_2 nanocomposite polyacrylonitrile films.

4. CONCLUSION

Surface-reinforced 8 wt% PAN-Fe_2O_3 and PAN-TiO_2 nonporous polyacrylonitrile membranes were successfully prepared for oil/water separation. One type, PAN-Fe_2O_3 and PAN-TiO_2, at 8 wt%, was used for testing its efficiency. The 8 wt% PAN-Fe_2O_3 and PAN-TiO_2, reinforced with 8 wt%, could effectively handle low oil and water concentrations. The optimum separation time was 5 min, after which the removal efficiency decreased with the 8 wt% PAN-Fe_2O_3 concentration. The best removal performance was achieved on the 8 wt% PAN-TiO_2 surfaces reaching 98% at a concentration of 10 g/90 mL (10 wt%) crude oil/water.

ACKNOWLEDGMENTS

We extend our sincere thanks to the Department of Chemical Engineering, College of Engineering, University of Baghdad, for their valuable support in completing this research project.

REFERENCE

[1] Abbas N. N., Mohammed A. H., Ahmad M. B. Copolymerization of Ethyl Methacrylate and Vinyl Acetate with Methacrylamide: Synthesis, Characterization and Reactivity Ratios. Egyptian Journal of Chemistry, 65(9), (2022). 293. https://doi.org/10.21608/ejchem.2022.112096.5091.

[2] A. M. Atta, H. S. Ismail, A. M. Elsaaed, Application of anionic acrylamide-based hydrogels in the removal of heavy metals from wastewater, J. Appl. Polym. Sci. 123 (2012) 2500–2510.

[3] J. Dickhut, J. Moreno, P. Biesheuvel, L. Boels, R. Lammertink, W. de Vos, Produced water treatment by membranes: a review from a colloidal perspective, J. Colloid Interface Sci. 487 (2017) 523–534.

[4] A. M. Atta, H. S. Ismail, A. M. Elsaaed, Application of anionic acrylamide-based hydrogels in the removal of heavy metals from wastewater, J. Appl. Polym. Sci. 123 (2012) 2500–2510.

[5] Abbas Sura Mawlood, and AL-Jubouri Sama Mohammed. ZrO_2 Nanoparticles Filler-Based Mixed Matrix Polyethersulfone/Cellulose Acetate Microfiltration Membrane for Oily Wastewater Separation. Applied Science and Engineering Progress, Vol. 18, No. 1, (2025), 7599.

[6] E. Karadağ, D. Saraydin, swelling of superabsorbent acrylamide/sodium acrylate hydrogels prepared using multifunctional crosslinkers, Turk. J. Chem. 26 (2002) 863–876.

[7] Assal Fatima Hekmat, Mohammed Ameen Hadi, Synthesis and characterizations of poly(hydroxybenzyl methacrylate-co-acrylamide) based hydrogel as drug delivery system, POLIMERY 2025, 70, nr 1.

[8] H.-A. Kalaleh, M. Tally, Y. Atassi, Preparation of Poly (sodium Acrylate-co-acrylamide) Superabsorbent Copolymer Via Alkaline Hydrolysis of Acrylamide Using Microwave Irradiation, Available: (2015) https://arxiv.org/ftp/arxiv/papers/1502/1502.03639.pdf.

[9] N. B. Shukla, G. Madras, Photo, thermal, and ultrasonic degradation of EGDMA crosslinked poly (acrylic acid-co-sodium acrylate-co-acrylamide) superabsorbent, J. Appl. Polym. Sci. 125 (2012) 630–639.

[10] Hidayah Malikhatu, Fitasari Dyah, Ma'ruf Anwar, Ruswan, Nadhifah. Synthesis and Characterization of Polyacrilonitrile-Fe_2o_3 Membrane Nano Composites for Oil Refinery Liquid Waste Separation. Advances in Engineering Research, volume 211, International Conference on Science and Engineering (ICSE-UIN-SUKA 2021).

[11] Isadora Dias Perez, Fernanda Brito dos Santos, Bianca Amos Estevam, João B.P. Soares, Melissa Gurgel Adeodato Vieira, Leonardo Vasconcelos Fregolente, Hydrogel-coated structured packing for water separation from oily liquid streams, Volume 305, 24 December (2024), 121135. https://www.sciencedirect.com/science/article/abs/pii/S0009250924014350?via%3Dihub.

[12] Teng Chen, Xin Xu, Jianqiang Hu, Li Guo, Shizhao Yang, Tianxiang Zhao, Jun Ma, Construction of heterostructure CoP/CN/Ni: Electron redistribution towards effective hydrogen generation and oxygen reduction, Chemical Engineering Journal Volume 415, 1 July (2021), 129031. https://www.sciencedirect.com/science/article/abs/pii/S1385894721006240.

[13] Estevam Bianca Ramos, Perez Isadora Dias, Ângela Aria Moraes, Leonardo Vasconcelos Fregolente, A review of the strategies used to produce different meshes in cellulose-based hydrogels, Materials Today Chemistry, Volume 34, December (2023), 101803.

[14] Blauth Sebastian, Stucke Dennis, Adel Ashour Mohamed, Schnebele Johannes, Grützner Thomas, Leithäuser Christian, CFD-based shape optimization of structured packings for enhancing separation efficiency in distillation, Chemical Engineering Science Volume 302, Part A, 5 February (2025), 120803.

[15] Hidayah Malikhatul, Fitasari Dyah, Ma'ruf Anwar, Ruswan, Nadhifah, Synthesis and Characterization of Polyacrilonitrile-Fe2o3 Membrane Nano Composites for Oil Refinery Liquid Waste Separation. *Advances in Engineering Research, volume 211 International Conference on Science and Engineering (ICSE-UIN-SUKA 2021).*

[16] Surkatti Riham, Loosdrecht Mark C. M. van, Hussein Ibnelwaleed A. and El-Naas Muftah H. PVA-TiO_2 Nanocomposite Hydrogel as Immobilization Carrier for Gas-to-Liquid Wastewater Treatment. *Nanomaterials* 2024, 14, 249. https://doi.org/10.3390/nano14030249.

[17] Salim S. H., Al-Anbari R. H., Haider A. 2022. Polysulfone/TiO_2 Thin Film Nanocomposite for Commercial Ultrafiltration Membranes," J. Appl. Sci. Nanotechnol., 2(1), 80–89. DOI: 10.53293/jasn.2022.4528.1121.

[18] Lu D. 2016. Hydrophilic Fe_2O_3 dynamic membrane mitigating fouling of support ceramic membrane in ultrafiltration of oil/water emulsion. Sep. Purif. Technol., 165, 1–9.

[19] Waghmode M. S., Gunjal A. B., Mulla J. A., Patil N. N., Nawani N. N. 2019. Studies on the titanium dioxide nanoparticles: Biosynthesis, applications, and remediation. SN Appl. Sci., 1(4), 1–9.

[20] Haider A., Al-Anbari R., Kadhim G., Jameel Z. 2018. Synthesis and photocatalytic activity of TiO2 nanoparticles for air purification. 2018 MATEC Web Conf., 162, 1–6. DOI: 10.1051/matecconf/201816205006.

[21] Alsalhy Q. F., Al-Ani F. H., Al-Najar A. E. 2018. A new Sponge-GAC-Sponge membrane module for submerged membrane bioreactor use in hospital wastewater treatment. Biochemical Engineering Journal, 133, 130–139.

[22] Amna J. S., Eman S. A., Kadhum M. Sh., Bassam I. Kh., Sama M., Sabirova T. M., Tretyakova N. A., Hasan S. M., Alsalhy Q. F., Auda J. B. 2020. Comparative study of embedded functionalised MWCNTs and GO in Ultrafiltration (UF) PVC membrane: interaction mechanisms and performance, International Journal of Environmental Analytical Chemistry.

[23] Aljumaily M., Alsaadi N. A., Alsalhy Q. F., Mjalli F. S., Atieh M. A. 2018. PVDF-co-HFP/superhydrophobic acetylene-based nanocarbon hybrid membrane for seawater desalination via DCMD. Chemical Engineering Research and Design, 138, 248–259.

[24] Aljumaily M., Alsaadi Hashim N. A., Alsalhy Q. F., Das R., Mjalli F. S. 2019. Embedded high-hydrophobic CNMs prepared by CVD technique with PVDF-co-HFP membrane for application in water desalination by DCMD, Desalination and Water Treatment, 142, 37–48.

[25] Amna J. S., Kadhum M. S., Bassam I. K., Alsalhy Q. F. 2020. Effect of embedding MWCNT-g-GO with PVC on the performance of PVC membranes for oily wastewater treatment. Chemical Engineering Communications, 207(6), 733–750.

[26] Rana J. K., Al-Ani Faris H., Alsalhy Q. F. 2021. MCM-41 mesoporous modified polyethersulfone nanofiltration membranes and their prospects for dyes removal, International Journal of Environmental Analytical Chemistry, 1–21.

[27] Reham R. A., Kadium M. S., Aseel B., Alsalhy Q. F. 2022. Novel photocatalytic polyether sulphone ultrafiltration (UF) membrane reinforced with oxygen-deficient Tungsten Oxide (WO2.89) for Congo red dye removal, Chemical Engineering Research and Design, 177, 526–540.

[28] Wu, J.; Yi, S.; Wang, Y.; Yao, J.; Gao, 2021, W. Polymer-based TiO_2 nanocomposite membrane: Synthesis and organic pollutant removal. Int. J. Smart Nano Mater. 12, 129–145.

[29] D. Maity, P. Chandrasekharan, F. Si-Shen, J. M. Xue, J. Ding, 2010, Polyol-based synthesis of hydrophilic magnetite nanoparticles. J. Appl. Phys. 107, 09B310.

[30] Suprihatin, I. E., Sibarani, J., Sulihingtyas, W. D., Ariati, K. 2019. Photodegradation of Remazol Brilliant Blue using Fe_2O_3 intercalated bentonite. Journal of Physics: Conference Series 1341(3):6–11. doi: 10.1088/1742 6596/1341/3/032028.

[31] H. Guo, P. Sun, Y. Liang, Y. Ma, Z. Qin, and S. Cui, 2014, n-situ Fabrication of Polyelectrolyte-CSH Superhydrophilic Coatings via Layer-by-Layer Assembly Chem. Eng. J., 253, 198–206.

[32] Mpelane, A., Katwire, D. M., Mungondori, H. H., Nyamukamba, P., Taziwa, R. T. 2020, Application of novel C-TiO_2-CFA/PAN photocatalytic membranes in the removal of textile dyes in wastewater. Catalysts, 10(8):1– 17. doi: 10.3390/catal10080909.

[33] Siwan Ghofran Qasem, Mohammed Ameen Hadi. 2024. Synthesis and characterization of multifunctional polymer additives for lubricating oils based on 2-ethylhexyl acrylate and N-isopropylmethacrylamide. POLIMERY, 69, nr 4.